

# QSO 0130-4021: A third QSO showing a low Deuterium to Hydrogen Abundance Ratio

David Kirkman<sup>1,2</sup>, David Tytler<sup>1,3</sup>,  
Scott Burles<sup>1,4</sup>

Dan Lubin<sup>1</sup> & John M. O'Meara<sup>1</sup>

Center for Astrophysics and Space Sciences;  
University of California, San Diego;  
MS 0424; La Jolla; CA 92093-0424

## ABSTRACT

We have discovered a third quasar absorption system which is consistent with a low deuterium to hydrogen abundance ratio,  $D/H = 3.4 \times 10^{-5}$ . The  $z_{abs} \sim 2.8$  partial Lyman limit system towards Q0130-4021 provides the strongest evidence to date against large D/H ratios because the H I absorption, which consists of a single high column density component with unsaturated high order Lyman series lines, is readily modeled – a task which is more complex in other D/H systems. We have obtained twenty-two hours of spectra from the HIRES spectrograph on the W.M. Keck telescope, which allow a detailed description of the Hydrogen. We see excess absorption on the blue wing of the H I Ly $\alpha$  line, near the expected position of deuterium. However, we find that Deuterium cannot explain all of the excess absorption, and hence there must be contamination by additional absorption, probably H I. This extra H I can account for most or all of the absorption at the D position, and hence  $D/H = 0$  is allowed. We find an upper limit of  $D/H \leq 6.7 \times 10^{-5}$  in this system, consistent with the value of  $D/H \simeq 3.4 \times 10^{-5}$  deduced towards QSO 1009+2956 and QSO 1937-1009 by Burles and Tytler (1998a, 1998b). This absorption system shows only weak metal line absorption, and we estimate  $[Si/H] \leq -2.6$  – indicating that the D/H ratio of

---

<sup>1</sup>Visiting Astronomer, W.M. Keck Observatory which is a joint facility of the University of California, the California Institute of Technology and NASA.

<sup>2</sup>E-mail: dkirkman@physics.bell-labs.com, present address: Bell Laboratories, Lucent Technologies, 600 Mountain Avenue, Murray Hill, NJ 07974-0636

<sup>3</sup>E-mail: tytler@ucsd.edu

<sup>4</sup>Present address: Univ. of Chicago, Astronomy & Astrophysics Center, 5460 S. Ellis Ave., Chicago, IL 60615

the system is likely primordial. All four of the known high redshift absorption line systems simple enough to provide useful limits on D are consistent with  $D/H = 3.4 \pm 0.25 \times 10^{-5}$ . Conversely, this QSO provides the third case which is inconsistent with much larger values.

## 1. Introduction

Big bang nucleosynthesis (BBN) is a cornerstone of modern cosmology. The standard theory (SBBN) predicts the abundances of the light nuclei (H, D,  $^3\text{He}$ ,  $^4\text{He}$ , and  $^7\text{Li}$ ) as a function of a single parameter, the cosmological baryon to photon ratio,  $\eta \equiv n_b/n_\gamma$  (Kolb & Turner 1990). The ratio of any two primordial abundances should yield a direct measurement of  $\eta$ , and the measurement of a third provides a test of the theory.

The abundances of all three of the light elements have been measured in a number of terrestrial and astrophysical environments, however, most of these are not primordial abundances, and corrections for later chemical evolution are problematic. Adams (1976) suggested that it might be possible to measure primordial D/H towards low metallicity absorption line systems in the spectra of high redshift QSOs. The task proved too difficult for 4-m class telescopes (Chaffee et al. 1985, 1986; Carswell et al. 1994), but became possible with the advent of the HIRES echelle spectrograph (Vogt 1994) on the W.M. Keck telescope. Using Keck+HIRES, Songaila et al. (1994) reported an upper limit of  $D/H < 25 \times 10^{-5}$  in the  $z_{abs} = 3.32$  Lyman limit system (LLS) towards QSO 0014+813. Using different spectra, Carswell et al. (1994) reported  $< 60 \times 10^{-5}$  in the same object, and they found no reason to think that the deuterium abundance might be as high as their limit. Chaffee et al. (1985, 1986) had reached the same conclusion a decade earlier. The most recent, improved spectra (Burles et al. 1999) support the early conclusions:  $D/H < 35 \times 10^{-5}$  for this QSO.

There are currently two known absorption systems in which D/H is low:  $D/H = 4.0 \pm_{-0.6}^{+0.8} \times 10^{-5}$  in the  $z_{abs} = 2.504$  LLS towards QSO 1009+2956 (Burles & Tytler 1998a), and  $D/H = 3.24 \pm 0.3 \times 10^{-5}$  in the  $z_{abs} = 3.572$  LLS towards QSO 1937-1009 (Tytler, Fan, and Burles 1996; Burles & Tytler 1998b).

There remains uncertainty over a fourth LLS at  $z_{abs} = 0.701$  towards QSO 1718+4807, because we lack spectra of the Lyman series lines which are needed to determine the velocity distribution of the Hydrogen. Webb et al. (1997a, 1997b) assumed a single hydrogen component and found  $D/H = 25 \pm 5 \times 10^{-5}$ . Levshakov et al. (1998) allow for non-Gaussian velocities and find

$D/H \sim 4.4 \times 10^{-5}$ , while Tytler et al. (1999) find  $8 \times 10^{-5} < D/H < 57 \times 10^{-5}$  (95%) for a single Gaussian component, or  $D/H$  as low as zero, if there are two hydrogen components, which is not unlikely.

Very few LLS have a velocity structure simple enough to show deuterium. This can be understood if the LLS arise in forming protogalaxies with potential wells of  $\sim 200 \text{ km s}^{-1}$ , as expected in most CDM hierarchical cosmologies (Cen and Ostriker 1993; Rauch et al. 1997). Since a merging protogalaxy is unlikely to make a simple absorption system, we usually see one or two absorbers with column densities  $N_{HI} > 10^{16} \text{ cm}^{-2}$  and several with  $N_{HI} > 10^{15} \text{ cm}^{-2}$  distributed over 200-300  $\text{km s}^{-1}$ . These absorbers usually absorb most of the QSO flux near  $-82 \text{ km s}^{-1}$  from  $\text{Ly}\alpha$ , where the D I line is expected, and hence we obtain no information of the column density of D I.

In this paper, we present a third absorption system which unambiguously shows low  $D/H$ . The  $z_{abs} = 2.799$  partial LLS towards Q0130-4021 is simpler than the others because the entire Lyman series is well fit by a single velocity component. The velocity of this component and its column density are well determined because many of its Lyman lines are unsaturated. Its  $\text{Ly}\alpha$  line is simple and symmetric, and can be fit, using zero free parameters, using only the H I parameters determined by the other Lyman series lines. There is barely enough absorption at the expected position of D to allow low values of  $D/H$ , and there appears to be no possibility of high  $D/H$ .

## 2. Observations and data reduction

Our observations of QSO Tololo 0130-403 (Osmer & Smith 1976; redshift 3.023,  $V=17.02$ , B1950 RA 1h 30m 50.3s, Dec  $-40^{\circ} 21' 51''$ ; J2000 1h 33m 1.96s  $-40^{\circ} 6' 28''$ ) with the HIRES echelle spectrograph on the W.M. Keck-I telescope are described in Table 1. We observed for 5 hours in 1995 and 1996 with the HIRES red cross disperser. This gave complete coverage between 3900 and 5200  $\text{\AA}$ , continuing from 5200 – 6000  $\text{\AA}$  with small ( $\sim 1 - 5 \text{ \AA}$ ) gaps every 40 – 50  $\text{\AA}$  between the spectral orders. We also observed for another 17.3 hours with the HIRES ultraviolet cross disperser, and obtained complete spectral coverage between 3350 and 4850  $\text{\AA}$ . All spectra used the HIRES C5 decker, which provides an entrance aperture to the spectrograph with dimensions  $7.5'' \times 1.15''$  and a spectral resolution of  $8 \text{ km s}^{-1}$ .

All observations were made at telescope elevations of less than  $30^{\circ}$  because of the low declination of the QSO. The UV observations were made with the parallactic angle aligned parallel to the spectrograph entrance slit using the

HIRES image rotator (Tytler et al. 1999), which was not available for the red observations.

The data were flat-fielded, optimally extracted, and wavelength calibrated in the standard way using Tom Barlow’s set of echelle extraction (EE) programs. Each observation was extracted and wavelength calibrated separately. The data were not flux calibrated, because this cannot readily be done to high accuracy. Instead, as described below, a local continuum was fit to each order of each observation.

### 2.1. Wavelengths

We performed several checks on the wavelength calibrations. For each spectral order, typically 20–30 Thorium or Argon reference lines were identified and hence we expect wavelength errors of  $< 0.1$  pixels. Several bright atmospheric OH emission lines were measured to lie within  $0.01 \text{ \AA}$  (about 0.04 pixels) of their expected positions.

The HIRES cross-disperser has been found to drift by up to a few pixels, especially when the telescope moves. Therefore, we obtained calibration spectra before and after each observation, but we found no shifts when we cross-correlated these images. We continuously monitored the position of the cross disperser, and we reset it when it moved, but we found no associated errors in wavelengths, in part because these shifts move spectra in the sky direction, along the length of the slit.

Each observation was rebinned onto a wavelength scale that was linear in velocity with  $2.1 \text{ km s}^{-1}$  pixels, and then combined into a single spectrum. Each pixel in the final spectrum is the weighted mean of the pixels values in each of the individual observations.

### 2.2. Continuum Placement

Low order continuum fits were used to avoid the introduction of artifacts. Prior to summation, a local continuum was fit to each order of each observation using the IRAF task CONTINUUM. A third order Legendre polynomial was fit to each order of each observation. This is a lower order than is needed to fully describe the continuum of a QSO over a HIRES echelle order. Kirkman and Tytler (1997) found that QSO continua regions with little absorption are typically described by a Legendre polynomial of order 7 to 9 per HIRES order. Here, we use third order polynomials for two reasons. First, they produce good

continuum levels throughout most of the spectrum, although there are some regions which may be off by  $\sim 10\%$ . Second, they give very similar continuum levels when applied to different observations of the same object, and hence they should not introduce artifacts when we combine the separate observations.

The IRAF CONTINUUM task was set to iterate until it found a stable fit, each time rejecting pixels more than  $1\sigma$  below the fit, and keeping all pixels above the fit. This set of rejection parameters results in the continuum task placing the continuum at the top of each order. The continuum task was allowed to fit each order of each observation without any operator supervision. This resulted in obviously incorrect continuum estimates in a number of locations throughout the each spectrum. Looking at the final combined spectrum, we checked the continuum level selected near each absorption feature discussed in this paper. With the exception of the region near the  $z_{abs} \sim 2.799$  H I Lyman limit, the automatically selected continuum is the same we would have chosen by eye, which is the standard way of continuum fitting QSO absorption line spectra. The procedure failed near the continuum discontinuity of the H I Lyman limit, but as anticipated, it failed in the same way in each of the individual observations and thus did not affect the shape of any of the absorption features. We hand corrected the continuum level in this region.

### 3. The $z_{abs} \sim 2.799$ partial Lyman Limit absorption system

Q0130-4021 has a partial Lyman limit absorption system at  $z_{abs} \sim 2.8$ . The lines associated with this system are tabulated in Table 2. This system is very simple, with only one major velocity component. We measure the H absorption and the D/H ratio first, and then the metal abundance.

#### 3.1. Hydrogen and Deuterium absorption

We can unambiguously determine the line parameters of the strongest Hydrogen absorbers by looking at the unsaturated high order Lyman series lines. Absorption from the Lyman series is shown in Figure 1. We have fit Voigt profiles to Ly-11, Ly-12 and Ly-13 using the VPFIT code (Webb 1987) to determine the H I absorption parameters of this system. These lines are all unsaturated and well fit by a single component at  $z = 2.799742$ . The column density,  $\log N_{HI} = 16.66 \pm 0.02 \text{ cm}^{-2}$ , is low, and the line width parameter  $b = 22.7 \pm 0.1 \text{ km s}^{-1}$  is narrow for a LLS. Figure 1 shows that the other Lyman series lines predicted by this fit are reasonable because they do not over absorb.

They frequently under absorb, which is not a problem, because we do not try to fit the Ly $\alpha$  forest absorption at other redshifts.

Figure 2 shows the H I Ly $\alpha$  line of the  $z \sim 2.8$  absorption system, overlaid with the fit predicted from the Lyman series lines Ly-11, Ly-12, and Ly-13, and three different values for D/H: 0,  $3.4 \times 10^{-5}$  and  $25 \times 10^{-5}$ . The saturated core and steep sides of the Ly $\alpha$  line are fit well, considering that no parameters were adjusted to fit the Ly $\alpha$ .

The parameters of the D I line are constrained by the H I. There should be a single D I component, because there is a single high column density H I component, and this D I must be at the same redshift as the H I. In the velocity frame of the H I, the D I line will be centered at  $-82 \text{ km s}^{-1}$ , or  $4617.976 \pm 0.004 \text{ \AA}$  (heliocentric, vacuum value).

We can readily estimate D/H by comparing the amount of absorption predicted with the spectra. The D/H = 0 under-absorbs near  $-82 \text{ km s}^{-1}$ , and hence there must be additional absorption, probably H or D. The D/H =  $3.4 \times 10^{-5}$  prediction is consistent with the data. However, additional absorption is needed near  $-70 \text{ km s}^{-1}$ , probably H I centered at  $-50 \text{ km s}^{-1}$ . Larger D/H does not help because it over-absorbs near  $-82 \text{ km s}^{-1}$ , as seen for D/H =  $25 \times 10^{-5}$ .

We draw four conclusions from Figure 2. First, no single line centered at  $-82 \text{ km s}^{-1}$  can account for all of the excess absorption from  $-100$  to  $-60 \text{ km s}^{-1}$ . Second, since the two (or more) lines are strongly blended it will be hard to partition the absorption between them, and hence we do not expect to make an accurate measurement of D/H. This is shown in Figure 3 where we see that residual optical depth after the removal of the main H is not clearly separated into two lines. Third, D/H <  $3.4 \times 10^{-5}$  is acceptable, and fourth, large values of D/H are strongly rejected.

We can place an interesting upper limit on the amount of D I present in this system because there is little absorption near  $-82 \text{ km s}^{-1}$ . We calculated a one sided  $\chi^2$  statistic between the observed data and the predicted H I + D I absorption as a function of D/H. For each pixel, the contribution to the one sided  $\chi^2$  is computed as a normal  $\chi^2$  statistic if the predicted flux lies below the data (i.e. if there is too much absorption, which is unphysical, and hence argues for rejection of the model) and is taken to be zero if the prediction lies above the data (which could be a result of unrelated absorption). We apply the statistic over the range  $4617 - 4618.3 \text{ \AA}$  (40 pixels), where the D line has the most effect on the fit. Since the value of  $N_{HI}$  was set using the higher order Lyman series lines, we can exclude wavelengths where H I is the main absorption, because

the quality of the fit in this region will have little effect on D/H. When D/H is zero, the fit lies above the data for nearly all pixels. As D/H increases the fit drops, and more pixels are included in the statistic. We calculated this statistic twice, once assuming  $b_{DI} = b_{HI}$  and again assuming  $b_{DI} = b_{HI}/\sqrt{2}$ , representing thermal broadening. The results are shown in Figure 4. The one sided  $\chi^2$  is essentially flat and constant for  $D/H < 4.5 \times 10^{-5}$ , and it increases rapidly with larger values of D/H. A value of  $D/H = 4.5 \times 10^{-5}$  is acceptable:  $\text{Prob}(\chi^2 > 20 \text{ for } 20 \text{ pixels}) = 0.45$ . The formal probabilities drop rapidly with increasing D/H, attaining  $\text{Prob}(\chi^2 > 48 \text{ for } 21 \text{ pixels}) = 0.0007$  by  $D/H < 5.4 \times 10^{-5}$ . We shall quote a limit of  $D/H < 4.8 \times 10^{-5}$  where the  $\text{Prob}(\chi^2 > 29 \text{ for } 20 \text{ pixels}) = 0.09$ . This limit is from random errors alone, assuming the continuum level shown in Figure 1. The 9% probability is an under-estimate because we ignored the 20 pixels which lie below the fit for this D/H value. If we were to add an additional absorption line to the fit of this wavelength region, and we assume that each of the ignored pixels then adds about unity to the  $\chi^2$  sum, then the 9% would change to about 18%.

We now discuss the continuum level errors, which are probably the dominant source of error since we are measuring a shallow (5% deep) D line in high signal to noise ratio spectra. There are few pixels near the continuum within  $300 \text{ km s}^{-1}$  of the D feature, which makes it difficult to estimate the error on the continuum level. From experience with similar spectra (Kirkman & Tytler 1997), we suggest that the continuum level error is about 2%, but we do not know how to estimate the distribution of this error with the existing data. The continuum could be higher than we have estimated, if the spectra near  $-150 \text{ km s}^{-1}$  and  $+190 \text{ km s}^{-1}$  are depressed by weak shallow Ly $\alpha$  absorption. If it were raised by 2%, there would be approximately 40% more optical depth at the position of the D line, and the upper limit on D/H would rise from  $< 4.8 \times 10^{-5}$  to  $< 6.7 \times 10^{-5}$ , which we consider to be similar to a  $1\sigma$  limit.

We cannot place a lower limit on the amount of D, because all the absorption at the position of D could be H. In the case of QSO 1009+2956 and QSO 1937-1009 (Tytler, Fan & Burles 1996; Tytler & Burles 1997; Burles & Tytler 1998b), we could use line widths to show that we had detected D. The absorption at the location of both those D lines was narrower than any normal Ly $\alpha$  forest line. But in the present case the absorption near D can be fit with  $b \simeq 22 \text{ km s}^{-1}$ , which is a common width for H in the Ly $\alpha$  forest.

### 3.2. Metal absorption

We detect metals at two velocities in this absorption system, Si III at  $v \sim 0$ , Si IV and C IV at  $v \sim -10$  km s<sup>-1</sup>, as shown in Figure 5. The properties of the detected ions are summarized in Table 2. The Si III line appears to be asymmetric, indicating that it may be a two component blend. However, we can only fit it as a single line because our data are not sufficient to deblend the two components. We did not detect any C II, Si II, C III, N V, O VI, or O I. C III could be present, but we cannot detect it because that region of the spectrum is strongly contaminated by unrelated Ly $\alpha$  forest absorption. The lack of C II and Si II is expected because the system is not optically thick at the H I Lyman limit: – C II and Si II are generally found only in gas that is shielded from the metagalactic UV background radiation below the H I Lyman limit. N V and O I are rarely observed, so the lack of absorption in these species is not surprising either.

The H I associated with the weak metal lines (C IV and Si IV) at  $v \sim -10$  km s<sup>-1</sup>, has a column density  $N_{HI} < 10^{16}$  cm<sup>-2</sup> because it is not seen in the high order Lyman series lines, especially Lyman-18, which are well fit with a single line at  $v = 0$ . Thus the conclusions of the last section are unaffected by the second velocity component at  $v \sim -10$  km s<sup>-1</sup>.

We estimate the metal abundance of the  $v = 0$  system by converting the observed column density ratio Si III/H I into [Si/H]. If we make the standard assumption that the absorber is in photoionization equilibrium with the metagalactic UV background, we need to determine the hydrogen density ( $n_H$ ) of the absorber and specify the spectrum of the UV background to make the conversion.

We get the  $n_H$  from numerical simulations of structure formation in CDM models. These often find a tight correlation between the  $N_{HI}$  of an absorption line, and  $n_H$  in the gas producing the absorption. Hellsten et al. (1997) found the relationship between column density and physical density to be well approximated by

$$\log n_H = -14.8 + \log \frac{\Omega_b h^2}{0.0125} + 0.7 \log N_{HI} \quad (1)$$

in simulations of both SCDM and LCDM Universes. Using  $\Omega_b h^2 = 0.019$  and  $\log N_{HI} = 16.66$  cm<sup>-2</sup>, we find that in this absorber, the predicted density is  $\log n_H = -2.9$  cm<sup>-3</sup>. Using CLOUDY (Ferland 1993) with a Madau spectrum for the metagalactic UV background, the observed [Si III/H I] implies [Si/H] = -2.6. If [C/Si]  $\sim 0.3$ , as in Population II stars, the solution is self consistent:



the predicted line strengths of O VI, C IV, Si IV, C II and Si II are low enough that they would not be detected in our data. The overall low metallicity of the system implies that the gas has not been reprocessed, and thus that our limit on D/H corresponds to gas which is primordial.

#### 4. Conclusions

To date, after the community has searched through more than 100 lines of sight, only four had previously been found with simple enough velocity structure to give useful limits on D/H. All four of these absorbers contain multiple strong H I velocity components. Two of the four yield a measurement of D/H, because they are free of major contamination, while the other two can be strongly contaminated, and allow  $D/H = 0$ .

Here we presented the fifth absorption system which is simple enough to show low D. The properties of the H are well determined. We find that  $D/H \simeq 3.4 \times 10^{-5}$  is acceptable, and that D/H ratios  $> 6.7 \times 10^{-5}$  are rejected. This absorber provides the strongest evidence yet against high D/H because it has unsaturated lines and the simplest velocity structure, with only a single major velocity component in H I. However, contamination by extra H absorption near the D position remains a problem, because a small column density of H I could readily explain all of the absorption near D. Hence  $D/H = 0$  is allowed.

The metallicity is apparently low, with  $[Si/H] \simeq -2.6$ , which implies that the D has not been destroyed in stars.

The limit  $D/H < 6.7 \times 10^{-5}$  is in agreement with our two other measurements of the primordial D/H:  $D/H = 4.0_{0.6}^{+0.8} \times 10^{-5}$  towards QSO 1009+2956 (Burles and Tytler 1998a) and  $D/H = 3.24 \pm 0.3 \times 10^{-5}$  towards QSO 1937-1009 (Tytler, Fan, and Burles 1996; Burles and Tytler 1998b). We have argued that two other QSOs, QSO 0014+813 (Burles et al. 1999) and QSO 1718+4807 (Tytler et al. 1999) are also consistent with this low D/H, and hence all QSO spectra are consistent with a low primordial D/H ratio,  $D/H \sim 3.4 \times 10^{-5}$ . However, QSOs 1009+2956 and 1937-1009 are inconsistent with  $D/H \geq 5 \times 10^{-5}$ , and now we have found that a third, Q0130-4021, is inconsistent with  $D/H \geq 6.7 \times 10^{-5}$ .

This work was funded in part by grant G-NASA/NAG5-3237 and by NSF grant 9420443. We are grateful to Steve Vogt, the PI for the Keck HIRES instrument, and to Theresa Chelminiak and Barbara Schaefer who helped us obtain the Keck spectra.

## REFERENCES

- Adams, T.F. 1976, A&A, 50, 461
- Burles, S. & Tytler, D. 1998a, ApJ, 507, 732
- Burles, S. & Tytler, D. 1998b, ApJ, 499, 699
- Burles, S., Kirkman, D. & Tytler, D. 1999, ApJ, 519, July 1
- Carswell, R. F., Rauch, M., Weymann, R. J., Cooke, A. J., & Webb, J. K. 1994, MNRAS, 268, L1
- Cen, R., and Ostriker, J.P. 1993, ApJ, 417, 404
- Chaffee, F. H., Foltz, C. B., Roser, H.-J., Weymann, R. J., & Latham, D. W. 1985, ApJ, 292, 362
- Chaffee, F. H., Foltz, C. B., Bechtold, J., & Weymann, R. J. 1986, ApJ, 301, 116
- Ferland, G. 1993, Univ. Kentucky Dept. Physics and Astron. Internal Rept.
- Hellsten, U., Hernquist, L., Katz, N., & Weinberg, D.H. 1998 ApJ 499, 172
- Kirkman, D., and Tytler, D. 1997, ApJ, 484, 672
- Kolb, E.W., and Turner, M.S. 1990, “The Early Universe”, Addison Wesley
- Levshakov, S.A., Kegel, W.H., & Takahara, F. 1998, A&A, 336, L29
- Osmer, P.S. & Smith, M.G. 1976, ApJ, 210, 267
- Rauch, M., Haehnelt, M.G., Steinmetz, M. 1997, ApJ, 481, 601
- Songaila, A., Cowie, L. L., Hogan, C. J., & Rugers, M. 1994, Nature, 368, 599
- Tytler, D., Fan, X.M., & Burles, S. 1996, Nature, 381, 207
- Tytler, D., Burles, S., Lu, L., Fan, X.M., Wolfe, A., & Savage, B.D. 1999, AJ, 117, 63
- Tytler, D., & Burles, S. 1997, in *Origin of Matter and Evolution of Galaxies* eds. T. Kajino, Y. Yoshii & S. Kubono (World Scientific Publ. Co.) (astro-ph 9606110) p37-63
- Vogt, S. S., et al. 1994, Proc. SPIE, 2198, 362
- Webb, J. 1987, Ph.D. thesis, University of Cambridge
- Webb, J. K., Carswell, R. F., Lanzetta, K. M., Ferlet, R., Lemoine, M., Vidal-Madjar, A., & Bowen, D. V. 1997a, Nature, 388, 250
- Webb, J. K., Carswell, R. F., Lanzetta, K. M., Ferlet, R., Lemoine, M., & Vidal-Madjar, A. 1997b, preprint, astro-ph 9710089



Table 1. Keck HIRES Spectra of Q0130-4021

Date	Cross Disperser	Exposure Time (s)	Wavelengths Covered (Å)	SNR 4620 Å <sup>a</sup>	SNR 3460 Å <sup>b</sup>
Dec. 1995	Red	7200	3650-6080	10	– <sup>c</sup>
Dec. 1996	Red	6400	3650-6080	8	– <sup>c</sup>
Dec. 1996	Red	4300	3650-6080	5	– <sup>c</sup>
Sep. 1998	UV	7200	3340-4880	25	8
Sep. 1998	UV	7200	3340-4880	25	9
Oct. 1998	UV	5400	3370-4910	20	6
Oct. 1998	UV	9000	3370-4910	29	10
Oct. 1998	UV	3900	3370-4910	15	4
Oct. 1998	UV	1800	3370-4910	4	1
Oct. 1998	UV	7200	3370-4910	13	4
Oct. 1998	UV	7200	3370-4910	12	3
Oct. 1998	UV	9000	3370-4910	20	6
Oct. 1998	UV	4438	3370-4910	12	4

<sup>a</sup>The  $z_{abs} \sim 2.8$  Ly $\alpha$  line falls at 4620 Å where the total signal to noise ratio is about 60 per 2.1 km s<sup>-1</sup>.

<sup>b</sup>The  $z_{abs} \sim 2.8$  Lyman limit falls at 3460 Å where the total signal to noise ratio is about 19 per 2.1 km s<sup>-1</sup>.

<sup>c</sup>The Red- cross-disperser observations of Q0130-4021 do not cover the  $z_{abs} \sim 2.8$  Lyman Limit

Table 2. Ions observed in the  $z \sim 2.8$  LLS towards Q0130-4021

Ion	$\log N$ ( $\text{cm}^{-2}$ )	$b$ ( $\text{km s}^{-1}$ )	$z$
H I	$16.66 \pm 0.02$	$22.7 \pm 0.1$	$2.799742 \pm 0.000003$
C IV	$12.77 \pm 0.08$	$6.1 \pm 0.9$	$2.799629 \pm 0.000010$
Si III <sup>a</sup>	$12.24 \pm 0.01$	$7.5 \pm 0.2$	$2.799736 \pm 0.000002$
Si IV	$12.33 \pm 0.03$	$6.5 \pm 0.7$	$2.799659 \pm 0.000006$

<sup>a</sup>The Si III line may be a two component blend.

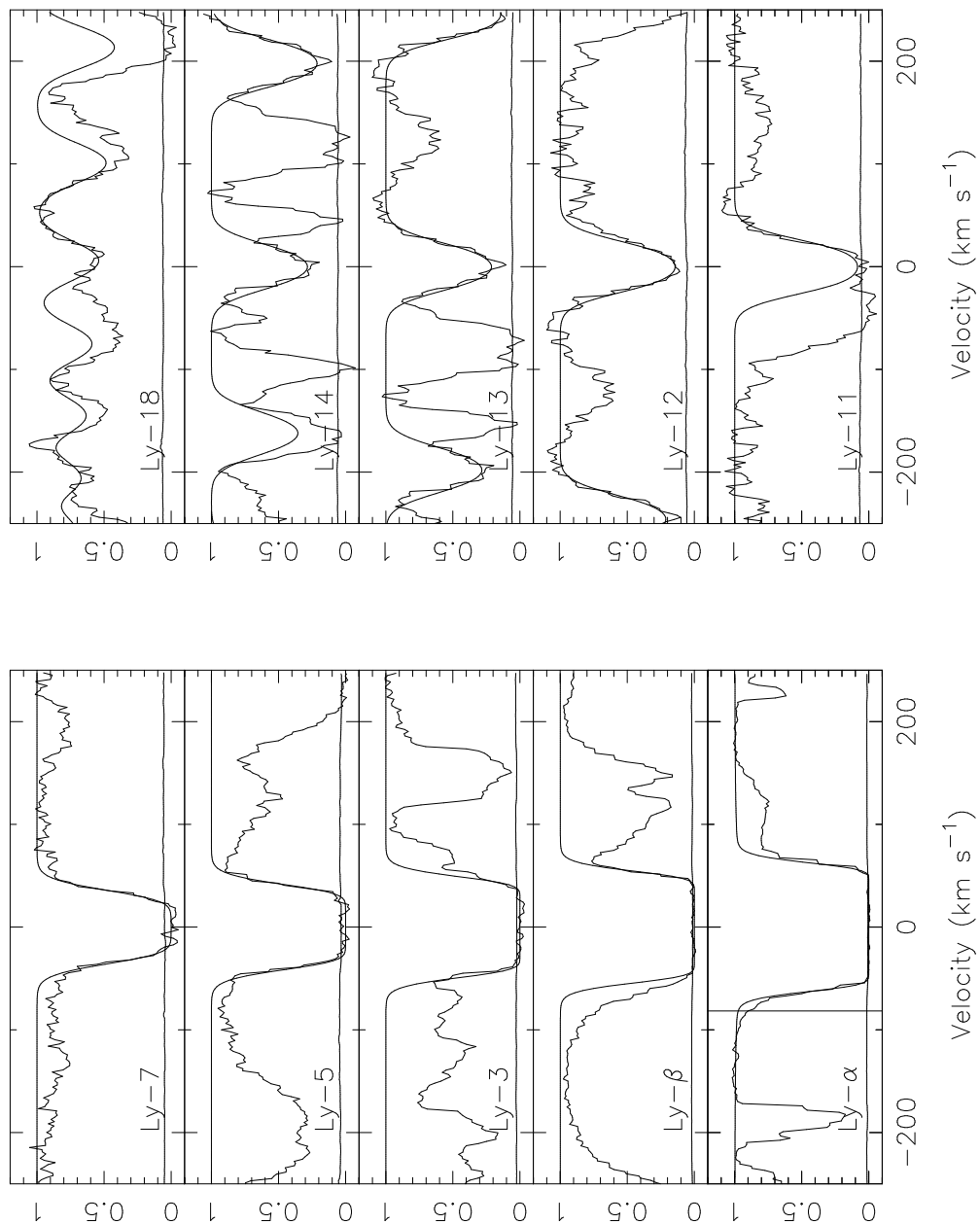


Fig. 1.— Lyman Series absorption in the  $z_{\text{abs}} \sim 2.8$  absorber. The smooth line is the fit to the H I, using the parameters in Table 2. The vertical line at  $-82 \text{ km s}^{-1}$  on the Ly $\alpha$  panel shows the expected position of D. The line just above zero in these and other spectral plots shows the  $1\sigma$  random error.

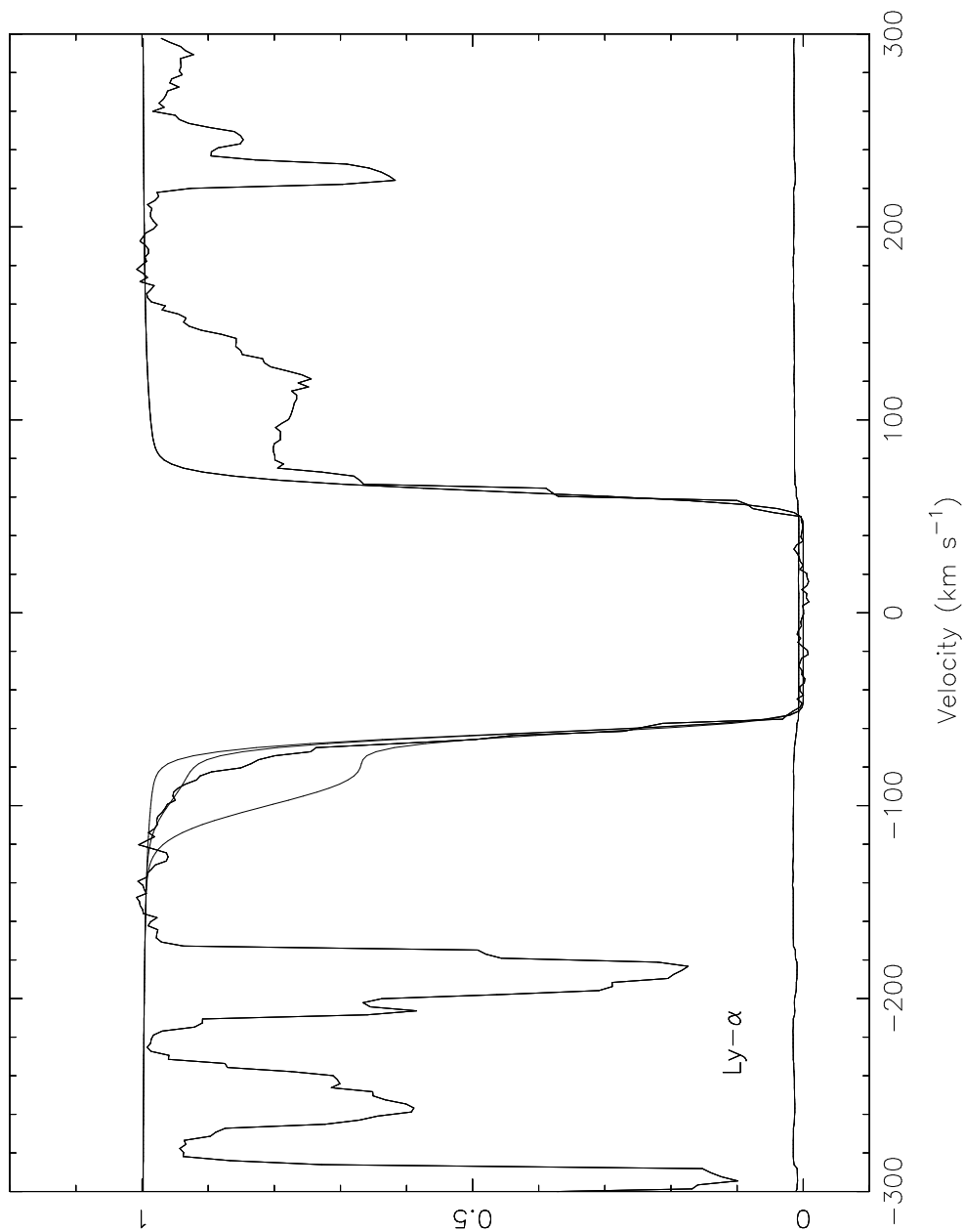


Fig. 2.— The Ly $\alpha$  line of the  $z_{abs} \sim 2.8$  LLS is centered at velocity  $v = 0 \text{ km s}^{-1}$ . The vertical line at  $-82 \text{ km s}^{-1}$  shows the expected position of D. Overlaid is the expected D+H absorption if  $D/H = 0$  (upper),  $D/H = 3.4 \times 10^{-5}$  (middle), and  $D/H = 25 \times 10^{-5}$  (lower), assuming turbulent broadening. The continuum level is at unity on the vertical scale.

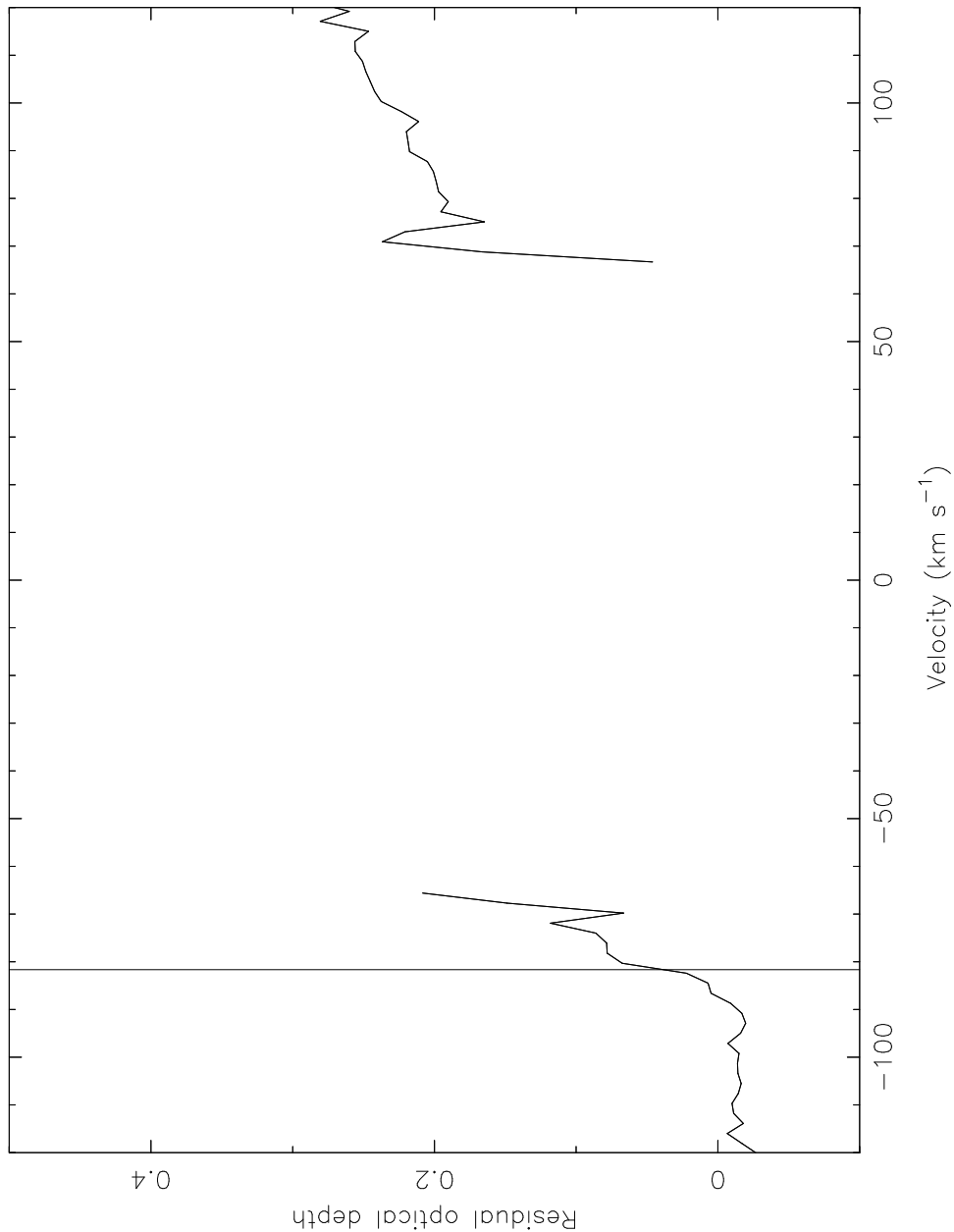


Fig. 3.— The excess absorption near the Ly $\alpha$  line of the  $z_{abs} \sim 2.8$  LLS. We plot the residual optical depth between the observed data and the H I line predicted from the higher order Lyman lines, using the parameters in Table 2. The residual optical depth is not symmetric about  $-82 \text{ km s}^{-1}$ , meaning that a D I line cannot fully explain all of the observed absorption on the blue wing of H I Ly $\alpha$ . The residual optical depth is poorly known, with large errors, near  $-65 \text{ km s}^{-1}$ , and is not known at  $-50 < v < +50 \text{ km s}^{-1}$  where we observe zero flux.



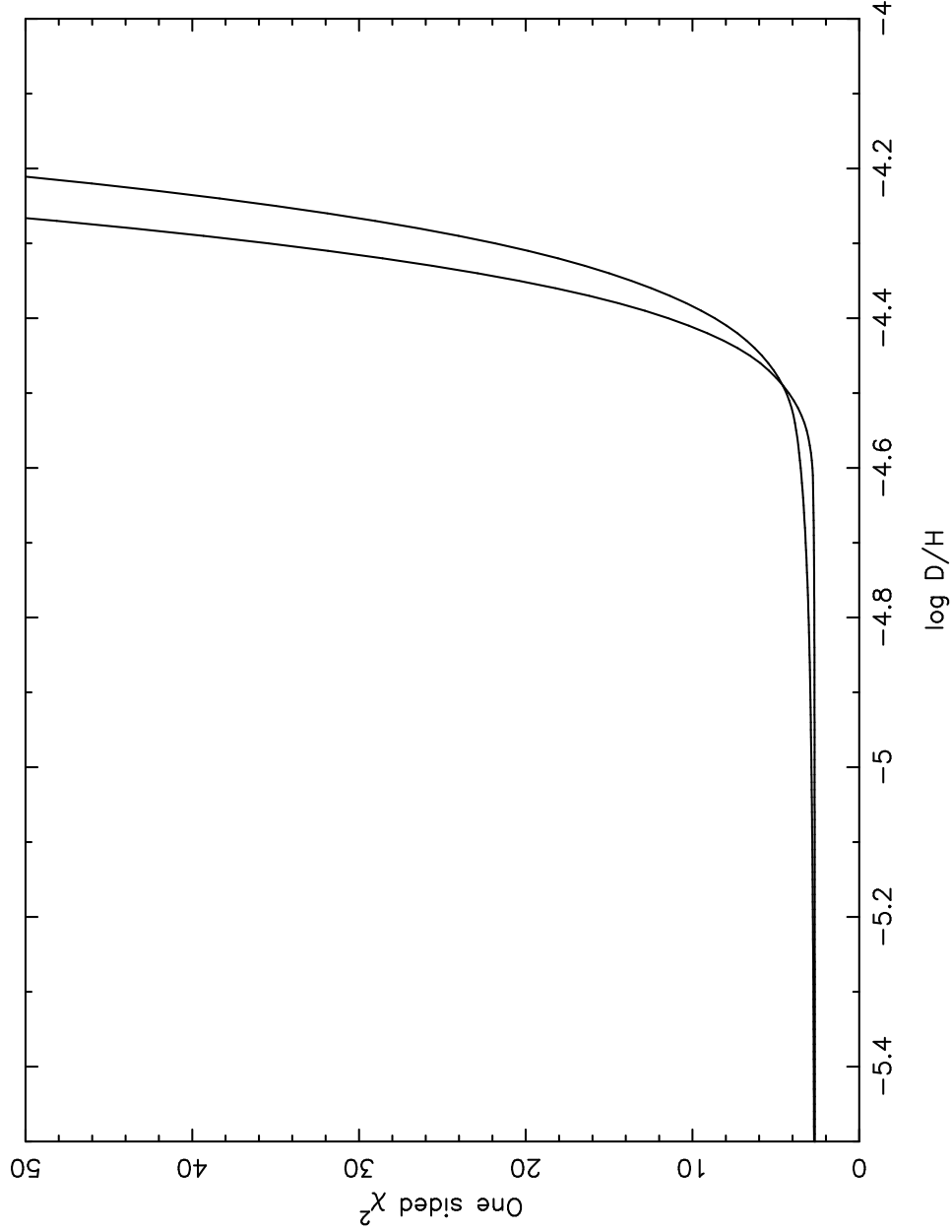


Fig. 4.— Goodness of fit of the model to the spectra in the region of the D line. We plot  $\chi^2$  vs D/H. The upper line (at  $\log D/H = -5$ ) assumes turbulent line widths, while the lower line assumes thermal line widths.

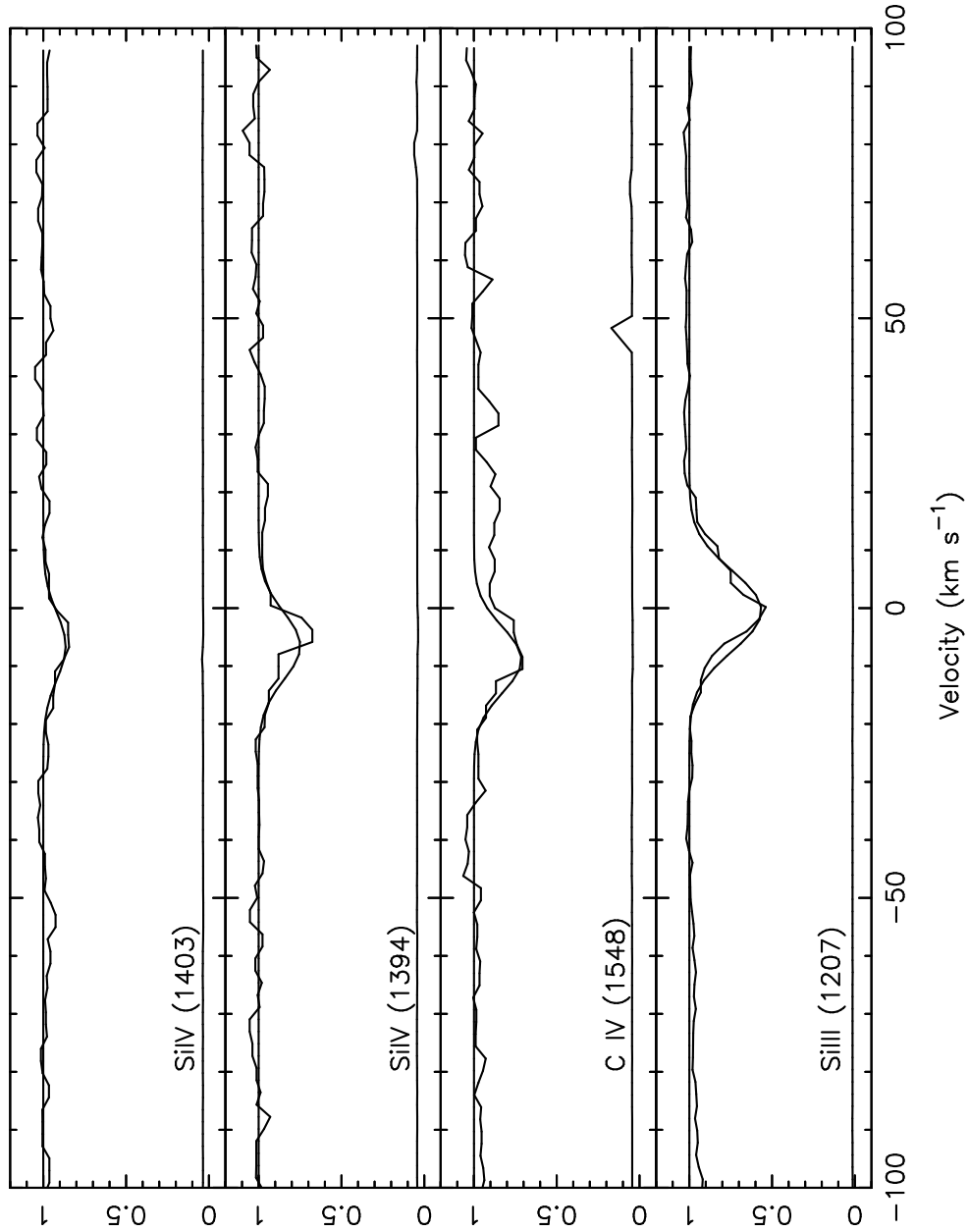


Fig. 5.— The metal absorption lines detected in the  $z_{abs} \sim 2.8$  absorber. Overlaid are the Voigt profiles fit to the absorption, using the parameters in Table 2.